Published in final edited form as:
Gene Ther. 2011 May ; 18(5): 432–436. doi:10.1038/gt.2010.153.

Air-assisted intranasal instillation enhances adenoviral delivery to the olfactory epithelium and respiratory tract

Philia Gau[*], **Steven Rodriguez, Ph.D**[*], **Christine De Leonardis**, **Patrick Chen**, and **David M. Lin, Ph.D**[1]
Department of Biomedical Sciences Cornell University Ithaca, NY 14853

Abstract

Intranasal instillation is used to deliver adenoviral vectors to the olfactory epithelium and respiratory tract. The success of this approach, however, has been tempered by inconsistent infectivity in both the epithelium and lungs. Infection of the epithelium may be hampered in part by the convoluted structure of the cavity, the presence of mucus, or poor airflow in the posterior cavity. Delivery of adenovirus to the lungs can be uneven in the various lobes, and distal bronchioles may be poorly infected. Current approaches to circumvent these issues rely principally on intubation or intratracheal instillation. Here we describe a technique that significantly improves adenoviral infectivity rates without requiring surgical intervention. We use compressed air to increase circulation of instilled adenovirus, resulting in enhanced infection in both the epithelium and lungs. This procedure is straightforward, simple to perform, and requires no specialized equipment. In the epithelium, neurons and sustentacular cells are both labeled. In the lungs, all lobes can be infected, with penetration to the most distal bronchioles. The use of compressed air will likely also be useful for enhancing the distribution of other, desired agents within the epithelium, CNS, and respiratory tract.

Keywords

intranasal instillation; olfactory; epithelium; lungs; adenovirus

Introduction

Intranasal instillation has been used to introduce adenoviruses, small molecules, drugs, and cells into the olfactory epithelium, CNS, and lungs[1-5]. The ease with which the nasal cavity can be accessed has made intranasal instillation an attractive means of manipulating gene expression. In the epithelium, adenoviral infection of olfactory sensory neurons (OSNs) has been used to study odorant receptor function, signal transduction, and growth cone proteins[1,6,7]. In the CNS, intranasal delivery can enable agents to bypass the blood-brain-barrier[8]. In the respiratory tract, intranasal introduction of gene therapy agents has been used to study cystic fibrosis and lung cancer[2,9].

In mice, simple intranasal instillation comprises pipetting an agent or adenoviral suspension on the naris and allowing the mouse to inspire the material. This procedure, however, has been hampered by variable infectivity and penetration. The highly convoluted structure of the mouse epithelium, the presence of mucus, or perhaps reduced airflow in the posterior

[1]To whom correspondence should be addressed dml45@cornell.edu Phone: 1-607-253-4360 Fax: 1-607-253-4212 .
[*]These authors contributed equally

The authors declare no competing financial interest.

reaches of the nasal cavity are thought to affect access of viruses, drugs, small molecules, and metals to OSNs and the CNS[10,11]. In the lungs, simple intranasal instillation can result in uneven distribution between the lobes and limited penetration of smaller airways[12].

A number of techniques have been proposed to improve upon the simple intranasal instillation protocol. The most commonly utilized approach involves intubation for the nasal epithelium[13] and intra-tracheal instillation for the lung[14]. These instillation procedures are generally quite successful, and can result in a high rate of infectivity. However, the procedures are invasive and can require specialized surgical training and equipment. Moreover, deposition of materials by intratracheal instillation can differ from that observed with normal inhalation[15].

Here we propose a technique that significantly improves adenoviral infectivity rates in both the epithelium and lungs. The approach involves the use of compressed air to augment simple intranasal instillation. The use of compressed air greatly improves circulation of inspired adenovirus in the nasal epithelium and respiratory tract, promoting increased infection without the need for surgical manipulation.

Results

Air-assisted intranasal instillation in the epithelium

To test the utility of our compressed air method, we used adenovirus expressing the *beta-galactosidase* gene from the CMV promoter (Ad-*lacZ*). For experiments involving infection of the olfactory epithelium, Ad-*lacZ* virus was diluted in methylcellulose, as studies have shown this vehicle improved infection of OSNs using lentiviral vectors[16].

Mice were anesthetized and adenovirus applied to the naris in 20 microliter aliquots. For no-air treated mice, the virus is simply inspired by the mouse. For air-assisted instillation, several puffs of compressed air are directed up the naris using a compressed air canister after instillation. This process is repeated two to three times until a total of 40-60 microliters of virus are delivered. Epithelial cryosections are then obtained after three to five days, and stained for *lacZ* activity. No-air and air-assisted epithelia are processed in parallel and stained for identical lengths of time.

A comparison of no-air and air-assisted epithelia shows a dramatic increase in *lacZ*-positive cells with the addition of compressed air (Fig. 1). Air-assisted animals also show infection of neurons that are difficult to access with no-air treatment. In particular, the dorsal recess of the epithelium (Fig. 1A, area between arrows) is almost never stained in no-air treated animals. In contrast, air-treated animals show heavy infection of the dorsal recess (Fig. 1B), although not all air-assisted animals always have this high expression in this area. This may be correlated with the age of the animal, as expression in this area tended to be somewhat better in younger mice.

At higher magnification, the pattern of *lacZ* staining indicates infection of both OSNs and sustentacular cells. The epithelium is a pseudostratified structure comprised of three major cell-types[17]. Sustentacular cells are glial-like cells that extend processes from the apical to basal surface. Sustentacular nuclei are typically located at the apical surface, adjacent to the lumen. OSNs are bipolar neurons that extend a dendrite to the apical surface and an axon basally. Their cell bodies are located within the middle layer of the epithelium, deep to sustentacular nuclei. Progenitor populations are located distal to the OSNs, and are adjacent to the basal lamina. The location of sustentacular cell nuclei can be easily detected by *in situ* hybridization using *cytokeratin 18* as probe[18] (Fig. 2A). Similarly, the location of mature OSNs can be detected using *olfactory marker protein (OMP)*[19] (Fig. 2C).

Infected sustentacular cells have strong staining in the apical epithelium, as well as labeled cellular processes that extend to the basal surface (Fig. 2B). In contrast, infected OSNs have strong expression in what appears to be cell bodies located within the neuronal layer. In many such cells, a thin process resembling a dendrite could be observed extending to the apical surface (Fig. 2D). Individual axons and axon bundles could also be detected in the lamina propria.

Adenoviral instillation volumes in various protocols range from 5 to 100 microliters at various titers[20]. We tested instillation with 40 or 60 microliters of virus at a titer of 10^{10} pfu/ml, and quantified the number of infected cells in each of the three major cell-types in the epithelium (Table 1). We found that few basal cells expressed *lacZ*. However, both OSNs and sustentacular cells are infected with either 40 or 60 microliter volumes. On average, the proportion of OSNs and sustentacular cells that are infected is approximately 50:50, although this varies between animals (Table 1). The reason for this variability is unclear, and does not appear to be related to the volume of adenovirus instilled.

We also assessed whether or not air-assisted mice exhibited higher levels of cell-death than non-air or sham treated animals. We performed terminal deoxynucleotide transferase-mediated dUTP nick end-labeling (TUNEL) on sections from sham treated animals (air-assisted animals instilled with vehicle only), no-air treated animals, and air-assisted animals (Table 2). All animals used for this analysis were instilled with 40 microliters of solution. Although a slight, upward trend is observed between the addition of adenovirus relative to vehicle only, and a further increase between the addition of air relative to no-air, these differences are not statistically significant.

We also tested other vectors using our approach. We infected animals with a *luciferase* adenovirus (Ad-*luc*). Sixty microliters of Ad-*luc* resuspended in methylcellulose was instilled with and without air. Luciferase activity was measured in epithelial lysates three days after instillation. In three separate pairs of mice instilled on three occasions, luciferase activity was higher in air-assisted animals relative to no-air animals (5.9-fold, 3-fold, and 2.1-fold, respectively). While the fold-change was apparent in all three experiments, there was variation both in the fold-change and in the absolute relative light units produced for each pair. However, even if RLU values are averaged for all three experiments, air-instilled animals still show a 2.3-fold increase in luciferase activity over no-air controls.

Air-assisted intranasal instillation in the respiratory tract

To determine the effectiveness of our approach within the lung, we again used the *Ad-lacZ* virus. For these experiments, saline was used as a vehicle instead of methylcellulose. No-air and air-assisted lungs infected with Ad-*lacZ* were reacted in parallel for identical lengths of time. No-air intranasal instillation produces weak *beta-galactosidase* activity in the lungs (Fig. 3A,C). Expression could be detected in both the left and right lobes, although the level and extent of expression was variable from animal to animal. In contrast, lungs in air-assisted instilled animals generally show dramatically elevated *lacZ* expression relative to no-air animals (Fig. 3B,D).

Although we see significantly elevated *lacZ* expression in air-assisted lungs relative to no-air lungs, penetration of adenovirus to the deepest bronchioles of the lung can be variable. In some animals, expression occurs in all bronchioles. In others, however, expression is not detected throughout the entire respiratory tree (Fig. 3B). Cryosections of *lacZ*-stained lungs show that expression could be weakly detected in no-air treated animals (Fig. 4A,C). In contrast, bronchioles in the proximal respiratory tract of air-assisted infected animals are strongly and uniformly stained (Fig. 4B). However, not all cells in the most distal respiratory

tract of air-instilled animals are stained (Fig. 4D). TUNEL analysis of lung tissue shows no significant cell death in either no-air or air-assisted animals (data not shown).

While Ad-*lacZ* is a useful means of assessing the utility of compressed air, an obvious extension of our protocol is to determine if it could be used in conjunction with the *cre-loxP* system. We therefore infected *rosa26stop-lacZ* animals[21] with Ad-*cre* virus. In *rosa26stop-lacZ* mice, expression of *beta-galactosidase* is controlled by the presence of *cre* recombinase. We stained lungs of animals infected with Ad-*cre* using our air-assisted protocol (Figure 5). We detected *lacZ* expression throughout the left and right lung in all lobes. The level of expression of *beta-galactosidase* did not appear to be quite as high as when adenovirus-*lacZ* alone was used to infect lungs. However, the expression of *lacZ* in these mice indicates that this approach can easily be used to drive expression of genes in the respiratory tree and epithelium using the *cre-loxP* system.

Discussion

Here we describe the use of compressed air to enhance adenoviral distribution after simple intranasal instillation. This straightforward procedure requires no specialized equipment or surgical manipulation, while significantly improving viral infectivity in both the epithelium and lungs. Furthermore, we found that our approach worked with three different adenoviruses (Ad-*lacZ*, Ad-*luc*, and Ad-*cre*). We therefore would expect our results to apply to other adenoviral expression vectors as well. In the epithelium, no-air instillation results in relatively poor infectivity of cells at the tested dose, and cells in the dorsal recess are often completely unaffected. In contrast, significant infection of the dorsal recess and epithelium can be detected in air-assisted animals. Furthermore, previous studies using a lentiviral luciferase vector showed that addition of methylcellulose increased luciferase activity levels approximately two-fold over using PBS alone[16]. Our results with luciferase adenovirus show a similar degree of improvement using air-assisted instillation.

In the lungs, no-air intranasal instillation of adenovirus results in weak *lacZ* activity. In contrast, air-assisted infected animals can show robust *lacZ* activity in all lobes with significantly improved infection of distal lung tissue. We also showed the use of air-assisted intranasal instillation can be used to drive expression of gene expression in the lungs in a conditional mouse mutant. By infecting animals bearing *loxP* conditional mutations with adenovirus-*cre*, it is possible to finely control temporal activation or inactivation of gene expression in the epithelium and respiratory tract.

There are aspects of this protocol that could be further optimized. Not all animals are equally infected in all tissues. While we were able to increase infectivity in the dorsal recess of the epithelium, these results were inconsistent. In some animals, the dorsal recess is heavily infected (e.g. Fig. 1), and in others, not at all. Regardless of the dorsal recess, infectivity of other areas as determined by *lacZ* activity was highly consistent, with broad distribution throughout the remainder of the nasal epithelium. Quantification showed that both sustentacular cells and OSNs were approximately equally infected, on average. To further manipulate the number of cells infected in the epithelium, higher titers of virus, further manipulating viscosity, pH, and other parameters, could also be tested to either increase or decrease infection. In the lungs, our approach improves infection relative to simple instillation. However, the deepest, most distal lung tissue can be inconsistently infected. Nevertheless, relative to no-air animals, expression of *beta-galactosidase* is strongly enhanced in the respiratory tract.

Our approach represents a straightforward yet powerful means of improving the delivery of molecules to the epithelium and lung. Because of the inconsistency associated with simple

intranasal instillation, various techniques have been developed to improve the delivery of viruses to the brain and lung. These include changing the viscosity of the delivery medium[16], using calcium phosphate solutions[22], employing nanoparticles[23], and the use of ultrasound to enhance DNA uptake[24]. Despite these innovative approaches, the most common approach has been to perform intubation to better access the nasal epithelium, or intratracheal instillation to infect the lung[7,14]. While intubation and intratracheal instillation are highly effective, they represent invasive approaches that can require surgical expertise. Our method requires no specialized technique or equipment, and yet achieves high infectivity rates in the epithelium and lung. The use of air to assist adenoviral infectivity therefore represents an easy but effective alternative to these more involved techniques.

Finally, it is possible to envision that air-assisted distribution will have utility beyond the use of adenovirus in gene therapy. Adenovirus is well-known to produce an inflammatory response in cells, and can lead to elevated levels of apoptosis[25]. For example, we observed slight increases in TUNEL-positive cells in air-assisted animals as compared with no-air animals, and both were slightly higher than vehicle only. While these differences were not significant, they may reflect the greater levels of infectivity observed in air-assisted animals, and a concomitant increase in issues associated with using adenovirus. To circumvent these potential side-effects, this approach could be tested with other viral vectors, including adeno-associated and retroviral-based systems. In addition, the use of air to improve circulation within the epithelium and lung could be used in combination with any of the other methods used to deliver drugs, DNA or proteins, such as incorporating cationic lipids or calcium phosphate in the delivery vehicle. The ability to easily and reproducibly increase penetration and access to the olfactory cavity and lungs will likely benefit studies aimed at ameliorating neurological and respiratory disease.

Materials and Methods

Mice

All animal protocols were approved by Cornell's IACUC. Mice ranged in age from one to four months of age, and were of a mixed 129SvEv/C57BL/6 or FVB background. *Rosa26stop-lacZ* mice[21] were used for adenovirus-*cre* experiments.

Sources of viral stocks

Ad5CMVcyto*lacZ* (Ad-*lacZ*; University of Iowa, Gene Transfer Vector Core, Iowa City, IA), Ad5CMV*luciferase* (Ad-*luciferase*; Gene Transfer Vector Core), or Ad5CMV*cre* (Ad-*cre*, a gift from the R. Weiss lab) was diluted to 10^{10} pfu/ml prior to instillation. For the olfactory epithelium, Ad-*lacZ* was diluted in 1% methylcellulose (Sigma-Aldrich, St. Louis, MO). For the lungs, Ad-*lacZ* or Ad-*cre* virus was diluted in saline.

Air-assisted delivery of adenovirus

Mice were anesthetized with avertin (Sigma-Aldrich), and adenovirus administered in 20 microliter aliquots. For each aliquot, the virus was first pipetted onto one naris and inspired by the mouse. After inspiration, air-assisted instillation was accomplished using a standard compressed air can (Whooshduster, VWR, Bridgeport, NJ). The snorkel of the compressed air canister was placed on the naris, and six to ten short bursts of air were administered after the virus had been inspired. The mouse's head was held steady during the air-assisted treatment, and then laid on its back for one to three minutes to allow the virus to adsorb. A total of 60 microliters of virus was delivered in three aliquots for all lung experiments, and 40-60 microliters was delivered for all olfactory epithelial experiments. For all no-air experiments, the same procedure was followed but without the addition of compressed air.

After recovery from anesthesia, mice were sacrificed three to five days following instillation.

LacZ staining

Whole mount lungs—Mice were euthanized and the lungs were perfused with 4% isotonic paraformaldehyde (PFA) containing 2mM $MgCl_2$. Lungs were removed, washed with PBS, and incubated in pre-staining solution (10mM PO_4 buffer pH 7.4 (Fisher, Pittsburg, PA), 150mM NaCl (Fisher), 1mM $MgCl_2$, 3mM $K_3Fe(CN_6)$ (Sigma-Aldrich), 3mM $K_4Fe(CN_6)$ (Sigma-Aldrich)) without X-gal (AllStar, Westerville, OH) at 37 °C. Staining solution with X-gal was prepared by adding 1/30 volume of 8% X-gal resuspended in dimethylformamide (Sigma-Aldrich) to prewarmed staining solution at 65 °C and then cooled to 37°C. Prestaining solution was replaced with staining solution with X-gal, and the lungs incubated at 37 °C. The reaction was quenched with 4% PFA and the tissue cleared in a sucrose gradient.

Olfactory epithelium—Epithelia were embedded in OCT (Sakura-FineTek, Torrance, CA), and fresh-frozen. Cryosections were fixed briefly with 2% isotonic PFA containing 2mM $MgCl_2$, washed with PBS, stained as described above. To quantify the location of *lacZ* expression, positive signals were counted from 7-10 sections per animal (for 40 or for 60 microliter instillation volumes, 8 animals were counted (four each no-air or air-assisted)).

Eosin staining—The accessory lobe of fixed, *lacZ*-stained lungs was embedded in OCT (Sakura-FineTek). Cryosections (20 microns) were fixed in 4% isotonic PFA, and washed sequentially with PBS, water, and 0.1% NH_4OH. Slides were stained with eosin (Fisher) and mounted. *LacZ* stained epithelial sections were similarly processed.

TUNEL—Fresh frozen cryosections (20 microns) were fixed in 4% isotonic PFA, washed with PBS, and incubated in precooled ethanol:glacial acetic acid (2:1) at −20 °C. Endogenous peroxidase activity was quenched with 3% hydrogen peroxide (Fisher). Sections were pre-incubated with equilibration buffer (Millipore, Billerica, MA) before addition of terminal transferase (New England Biolabs (NEB), Ipswich, MA) in incubation buffer (1× CoCl2 (NEB), 1× restriction buffer 4 (NEB), 0.5 nM biotin–dUTP (Roche, Nutley, NJ)), and incubated for 3.5 h at 37 °C. The transferase reaction was stopped with PBS containing 100mM EDTA and the sections incubated with streptavidin–HRP (Invitrogen, Carlsbad, CA). Reaction product was generated using the AEC kit (Invitrogen). To quantify the TUNEL data, positive signals were counted from five to ten sections per animal to determine the number of positive signals per section and standard error. Sham treated animals were instilled with methylcellulose that did not contain Ad-*lacZ* using our air-assisted approach.

In situ* hybridization—In situ* hybridization was performed as previously described[17]. Probes corresponded to the following regions for each gene: *cytokeratin 18* (nt 1-1400 of NM_010664); *OMP* (IMAGE clone IRAKp961I03127Q).

Luciferase activity measurements—Infected epithelia were removed three days after infection and homogenized using a TissueLyser (Qiagen, Valencia, CA) in cell culture lysis buffer (Promega, Madison, WI). Lysates were cleared by centrifugation and the supernatant stored at −80°C. Lysate protein was normalized by BCA protein assay (Pierce, Pittsburgh, PA) and luciferase activity measured using Promega's luciferase assay kit. Luciferase substrate was mixed with 25 or 50 μg of protein and relative light units determined with a Lumat luminometer (Berthold, Bad Wildbad, Germany) set for 10 second measurements with a two second delay. Uninfected epithelial lysate was used as a negative control.

Acknowledgments

We thank Stephanie Yaszinski for assistance with perfusion and dissection of the lungs, and the Weiss lab for the Ad-*cre* virus. We thank the Roberson lab for use of the luminometer. DML was supported by NIH DC007489, AG033241, and the Alzheimer's Association.

References

1. Chesler AT, Zou DJ, Le Pichon CE, Peterlin ZA, Matthews GA, Pei X, et al. A G protein/cAMP signal cascade is required for axonal convergence into olfactory glomeruli. Proc Natl Acad Sci U S A. 2007; 104:1039–1044. [PubMed: 17215378]
2. Crystal RG, McElvaney NG, Rosenfeld MA, Chu CS, Mastrangeli A, Hay JG, et al. Administration of an adenovirus containing the human CFTR cDNA to the respiratory tract of individuals with cystic fibrosis. Nat Genet. 1994; 8:42–51. [PubMed: 7527271]
3. Damjanovic D, Zhang X, Mu J, Medina MF, Xing Z. Organ distribution of transgene expression following intranasal mucosal delivery of recombinant replication-defective adenovirus gene transfer vector. Genet Vaccines Ther. 2008; 6:5. [PubMed: 18261231]
4. Danielyan L, Schafer R, von Ameln-Mayerhofer A, Buadze M, Geisler J, Klopfer T, et al. Intranasal delivery of cells to the brain. Eur J Cell Biol. 2009; 88:315–324. [PubMed: 19324456]
5. Dhuria SV, Hanson LR, Frey WH 2nd. Intranasal drug targeting of hypocretin-1 (orexin-A) to the central nervous system. J Pharm Sci. 2009; 98:2501–2515. [PubMed: 19025760]
6. Holtmaat AJ, Hermens WT, Sonnemans MA, Giger RJ, Van Leeuwen FW, Kaplitt MG, et al. Adenoviral vector-mediated expression of B-50/GAP-43 induces alterations in the membrane organization of olfactory axon terminals in vivo. J Neurosci. 1997; 17:6575–6586. [PubMed: 9254670]
7. Zhao H, Ivic L, Otaki JM, Hashimoto M, Mikoshiba K, Firestein S. Functional expression of a mammalian odorant receptor. Science. 1998; 279:237–242. [PubMed: 9422698]
8. Dhuria SV, Hanson LR, Frey WH 2nd. Intranasal delivery to the central nervous system: mechanisms and experimental considerations. J Pharm Sci. 2010; 99:1654–1673. [PubMed: 19877171]
9. Bridle BW, Boudreau JE, Lichty BD, Brunelliere J, Stephenson K, Koshy S, et al. Vesicular stomatitis virus as a novel cancer vaccine vector to prime antitumor immunity amenable to rapid boosting with adenovirus. Mol Ther. 2009; 17:1814–1821. [PubMed: 19603003]
10. Mathison S, Nagilla R, Kompella UB. Nasal route for direct delivery of solutes to the central nervous system: fact or fiction? J Drug Target. 1998; 5:415–441. [PubMed: 9783675]
11. Zhao H, Otaki JM, Firestein S. Adenovirus-mediated gene transfer in olfactory neurons in vivo. J Neurobiol. 1996; 30:521–530. [PubMed: 8844515]
12. Ganguly S, Moolchandani V, Roche JA, Shapiro PS, Somaraju S, Eddington ND, et al. Phospholipid-induced in vivo particle migration to enhance pulmonary deposition. J Aerosol Med Pulm Drug Deliv. 2008; 21:343–350. [PubMed: 18823258]
13. Holtmaat AJ, Hermens WT, Oestreicher AB, Gispen WH, Kaplitt MG, Verhaagen J. Efficient adenoviral vector-directed expression of a foreign gene to neurons and sustentacular cells in the mouse olfactory neuroepithelium. Brain Res Mol Brain Res. 1996; 41:148–156. [PubMed: 8883946]
14. DuPage M, Dooley AL, Jacks T. Conditional mouse lung cancer models using adenoviral or lentiviral delivery of Cre recombinase. Nat Protoc. 2009; 4:1064–1072. [PubMed: 19561589]
15. Driscoll KE, Costa DL, Hatch G, Henderson R, Oberdorster G, Salem H, et al. Intratracheal instillation as an exposure technique for the evaluation of respiratory tract toxicity: uses and limitations. Toxicol Sci. 2000; 55:24–35. [PubMed: 10788556]
16. Sinn PL, Burnight ER, Hickey MA, Blissard GW, McCray PB Jr. Persistent gene expression in mouse nasal epithelia following feline immunodeficiency virus-based vector gene transfer. J Virol. 2005; 79:12818–12827. [PubMed: 16188984]
17. Rodriguez S, Sickles HM, Deleonardis C, Alcaraz A, Gridley T, Lin DM. Notch2 is required for maintaining sustentacular cell function in the adult mouse main olfactory epithelium. Dev Biol. 2008; 314:40–58. [PubMed: 18155189]

18. Suzuki Y, Takeda M. Keratins in the developing olfactory epithelia. Brain Res Dev Brain Res. 1991; 59:171–178.

19. Margolis FL. Olfactory marker protein (OMP). Scand J Immunol Suppl. 1982; 9:181–199. [PubMed: 6963760]

20. Southam DS, Dolovich M, O'Byrne PM, Inman MD. Distribution of intranasal instillations in mice: effects of volume, time, body position, and anesthesia. Am J Physiol Lung Cell Mol Physiol. 2002; 282:L833–839. [PubMed: 11880310]

21. Soriano P. Generalized lacZ expression with the ROSA26 Cre reporter strain. Nat Genet. 1999; 21:70–71. [PubMed: 9916792]

22. Fasbender A, Lee JH, Walters RW, Moninger TO, Zabner J, Welsh MJ. Incorporation of adenovirus in calcium phosphate precipitates enhances gene transfer to airway epithelia in vitro and in vivo. J Clin Invest. 1998; 102:184–193. [PubMed: 9649572]

23. Teijeiro-Osorio D, Remunan-Lopez C, Alonso MJ. New generation of hybrid poly/oligosaccharide nanoparticles as carriers for the nasal delivery of macromolecules. Biomacromolecules. 2009; 10:243–249. [PubMed: 19117404]

24. Xenariou S, Griesenbach U, Liang HD, Zhu J, Farley R, Somerton L, et al. Use of ultrasound to enhance nonviral lung gene transfer in vivo. Gene Ther. 2007; 14:768–774. [PubMed: 17301842]

25. Brand K, Klocke R, Possling A, Paul D, Strauss M. Induction of apoptosis and G2/M arrest by infection with replication-deficient adenovirus at high multiplicity of infection. Gene Ther. 1999; 6:1054–1063. [PubMed: 10455408]

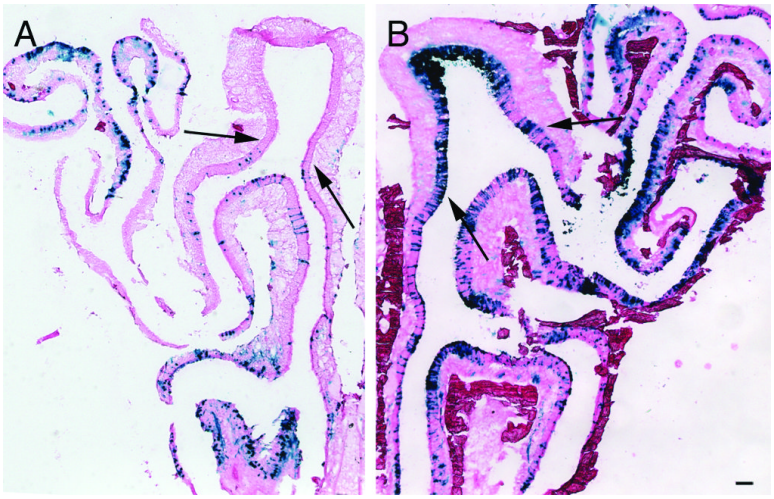

Figure 1.

No-air and air-assisted infected epithelia

A) Cryosections of no-air and B) air-assisted epithelium infected with Ad-*lacZ* and counterstained with eosin. Air-assisted epithelia (n=9) show significantly increased rates of infection throughout the epithelium compared to no-air (n=6). Expression can also be detected in the dorsal recess (compare area between black arrows in (A) and (B)). Scale bar = 100 μm.

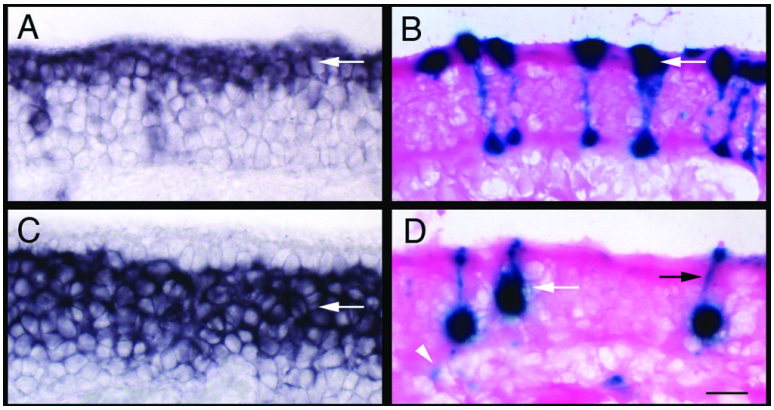

Figure 2.

Infection of sustentacular cells and OSNs by Ad-*lacZ*

A) *In situ* hybridization with *cytokeratin 18*, which labels sustentacular cells primarily at the apical surface (arrow). B) *LacZ* activity detected in the sustentacular layer in Ad-*lacZ* infected mice. Infected cells have processes that extend to the basal surface (arrow). C) *In situ* hybridization with *OMP*, which labels mature OSNs (arrow). D) *LacZ* activity detected in cells located within the olfactory nerve layer (white arrow). Dendritic processes of OSNs extending to the apical surface (black arrow) as well as axonal projections (white arrowhead) can be detected. Scale bar = 20 μm.

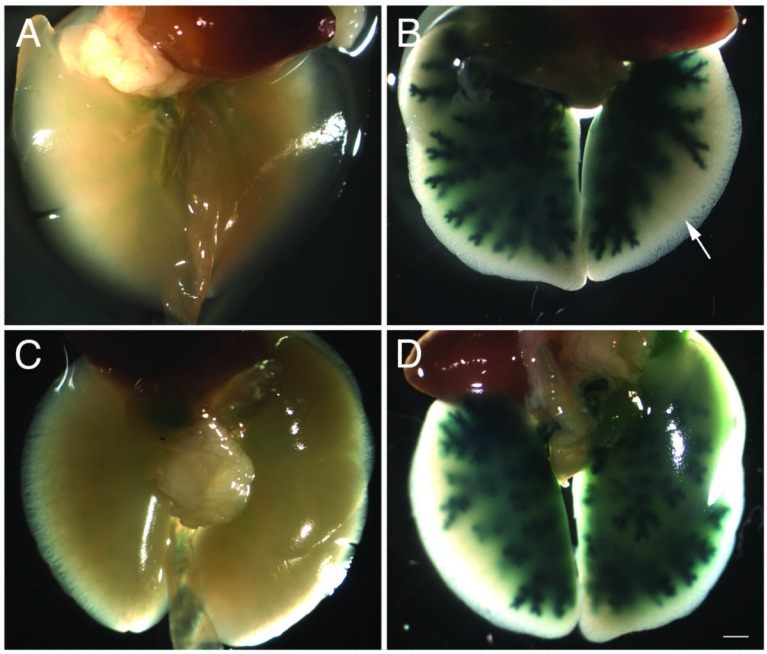

Figure 3.

No-air and air-assisted infected lungs

A) Ventral view of the lungs of an animal infected with Ad-*lacZ* using the no-air instillation method (n=4). B) Ventral view of the lungs of an animal infected with Ad-*lacZ* using the air-assisted instillation method (n=4). Note *lacZ* expression does not always extend to the most distal bronchioles (arrow) in all air-assisted animals. C) Dorsal view of same lungs shown in (A). D) Dorsal view of same lungs shown in (B). Scale bar = 100 μm.

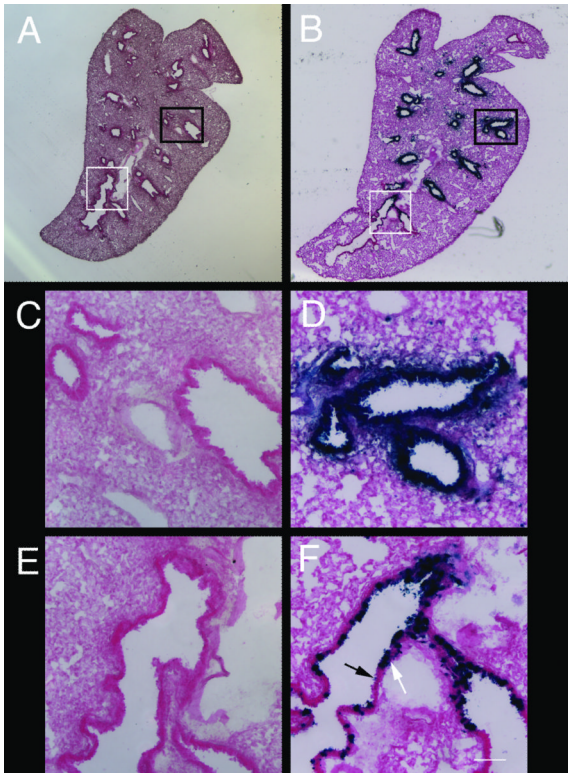

Figure 4.

Infection of proximal and distal respiratory tract by Ad-*lacZ*

A) Cryosection of lungs from an animal infected with Ad-*lacZ* using the no-air instillation method. B) Cryosection of an animal infected using the air-assisted method. C) Area in (A) outlined by black box. D) Area in (B) outlined by black box. E) Area in (A) outlined by white box. F) Area in (B) outlined by white box. Variability in *lacZ* staining is observed in the most distal bronchioles (F), with stained (white arrow) and unstained (black arrow) cells. *LacZ* staining could be seen in these sections from no-air instilled animals (C,E), but the expression was extremely weak. Scale bar = 640 μm (A,B) and 100 μm (C-F).

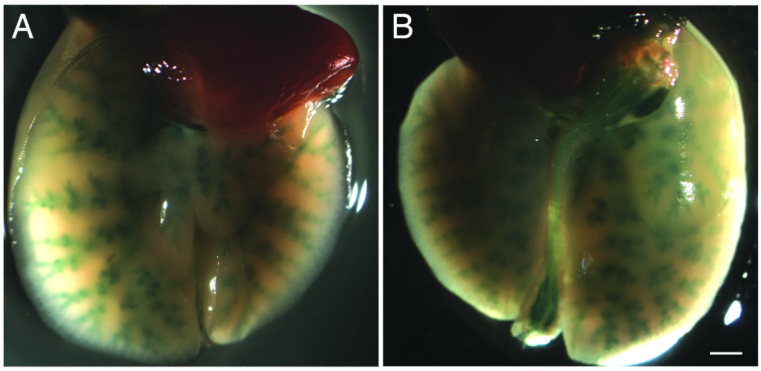

Figure 5.

Ad-*cre* driven expression of *beta-galactosidase*

A) Ventral view of lungs from an animal infected with Ad-*cre* (n=4) using the air-assisted instillation method. B) Dorsal view of same sample shown in (A). Note in this animal *lacZ* activity can be detected in what appears to be the entire tracheal tree. Scale bar =100 μm.

Table 1

Quantitation of *lacZ*-positive cells in animals infected with 40 or 60 μl of Ad-*lacZ* (n=4 per condition).

	number counted			
treatment	**#1**	**#2**	**#3**	**#4**
40ul - OSNs	128	83	163	82
40ul - Sust.	54	68	68	46
60ul - OSNs	54	69	67	54
60ul - Sust.	87	23	63	43

Table 2

Quantitation of TUNEL-positive cells in sham (vehicle plus air-assisted), no-air, and air-assisted animals (n=3 per condition).

	cells counted				
treatment	**#1**	**#2**	**#3**	**avg spots/section**	**std error**
sham	236	333	297	34.6	2.33
no air	363	218	389	35.9	2.54
air	312	323	186	39.1	2.12